^{13}C NMR Investigation of Local Dynamics in Compatible Polymer Blends

C. Le Menestrel, A. M. Kenwright,† P. Sergot, F. Lauprêtre,* and L. Monnerie

Laboratoire de Physico-Chimie Structurale et Macromoléculaire associé au CNRS, ESPCI, 10 rue Vauquelin, 75 231 Paris Cedex 05, France

Received April 25, 1991; Revised Manuscript Received January 22, 1992

ABSTRACT: Compatible blends of polystyrene and poly(vinyl methyl ether) have been studied by high-resolution solid-state ^{13}C NMR. Line widths and spin–lattice relaxation times in the rotating frame have been measured for different resonances as a function of both temperature and blend composition. Results thus obtained have shown the existence of local chain motions with different frequencies and temperature dependences for the two polymers. By varying the blend composition, it has been possible to investigate the influence of intermolecular interactions on the local chain dynamics of both components.

The local dynamics of polymers has been studied by a number of techniques. However, up until now, little was known about the local motions of individual chains in a compatible polymer blend. An interesting question to be addressed is the following: Do the two components of a compatible blend share the same local chain dynamics, i.e., are they involved in motions characterized by the same frequency and temperature dependence, or is it the opposite situation where each component has its own behavior? The answer to this question deals with a much more general problem than the precise behavior of polymer blends. It is related to the relative role of intramolecular constraints and intermolecular interactions in determining the nature and rate of molecular motions. In this respect, compatible blends are of special interest since, in a blend of two given compatible homopolymers, the intramolecular constraints are constant, fixed by the chemical structure of the components independently of the blend composition, whereas the intermolecular interactions depend on the blend composition. Therefore, the study of compatible blends as a function of their composition should lead to a deeper understanding of the influence of these two contributions on the local dynamics not only in the case of blends but also in the larger field of bulk polymers.

In this paper, we will examine the local dynamics of the polystyrene (PS) and poly(vinyl methyl ether) (PVME) chains in a series of compatible PS/PVME blends with different compositions. The technique used is high-resolution solid-state ^{13}C NMR. Its major advantage in the present investigation is its selectivity, i.e., its ability to observe separately the behavior of both components. Very recently, and independently of our work, results obtained on PS/PVME blends by high-resolution solid-state ^{13}C NMR have been reported by Takegoshi and Hikichi.[1] However, because of instrumental limits, they did not fully characterize the PS local motions, and, therefore, the effects of blending on molecular motions were mainly investigated through the study of the local dynamics of the PVME chains.[1]

† Present address: Interdisciplinary Research Centre in Polymer Science and Technology, University of Durham, Durham DH1 3LE, U.K.

Experimental Section

Although compatible over a large temperature range, the polystyrene/poly(vinyl methyl ether) blends have a lower critical solution temperature (LCST). As the precise shape of the phase diagram depends on the molecular weight and polydispersity of the polymers, the homopolymer samples under study have been chosen in such a way that the resulting blends are compatible over the whole temperature range (from −30 to +120 °C) of the NMR experiments. Results reported in ref 2 for a PVME of M_w = 99 000 have shown that a LCST of 150 °C is obtained for a value M_w = 27 800 of the molecular weight of the polystyrene. Blends based on PVME with M_w = 99 000 and polystyrene with a molecular weight lower than 27 800 have a higher LCST. Therefore, the characteristics of the homopolymers used in this study were the following: for the PS sample, purchased from Interchim, M_n = 19 160 and M_w = 22 760, and for the PVME sample, purchased from Scientific Polymer Products, Inc., M_n = 46 500 and M_w = 99 000. The tacticity of PVME was determined using high-resolution ^{13}C NMR in solution. The percentages of meso (m) and racemic (r) diads were found to be 37 and 63%, respectively.

Homogeneous blends of PS and PVME were prepared by freeze-drying 10% w/w solutions in benzene. Blends thus obtained were dried under vacuo for 24 h at room temperature and then at 60 °C at reduced pressure under nitrogen for another 24 h to effect complete removal of the solvent. In this way, samples containing 38, 52, and 67 wt % PS were prepared. In these samples, only one glass–rubber transition temperature, $T_{g\ blend}$, as measured by DSC at 20 °C/min, was observed, which reflects the homogeneous character of the blends at the molecular level. The values obtained for $T_{g\ blend}$ were −19, −6, and +19 °C, for the 38, 52, and 67 wt % PS samples, respectively.

Most high-resolution solid-state ^{13}C NMR spectra were obtained using the combined techniques of cross-polarization (CP), proton dipolar decoupling (DD), and magic-angle spinning (MAS)[3] at the operating frequencies of 25.15 and 75.47 MHz on Bruker CXP 100 and CXP 300 spectrometers, respectively. The strength of the ^{13}C and ^{1}H fields used to effect cross-polarization was 63 kHz. Contact durations were either 1 ms (normal cross-polarization experiments) or 20 μs (cross-polarization experiments with very short contact times). Some direct polarization (DP) experiments with 60-s recycle delays were also performed at high temperature. Variable-temperature experiments at 75.47 MHz were made by using a Doty probe. The spinners were of the cylindrical double-bearing type and were made from alumina. Measurements were carried out at temperatures lower than 130 °C to avoid system fluctuations on approaching the LCST. At 75.47 MHz, the spinning rate was chosen in such a way as to avoid as much as possible the presence of spinning side bands associated with the PS aromatic ^{13}C resonances at the site of the PVME methine carbon line. It was in the range from 4000 to

0024-9297/92/2225-3020$03.00/0

4800 Hz depending on the temperature and the spectrometer. Spin-temperature inversion[4] and flip-back[5] were employed systematically throughout. ^{13}C spin-lattice relaxation times in the rotating frame were measured using the carbon spin-locking sequence described in ref 3 and recording the signal intensities as a function of the variable time, Δt, during which the carbons are held in their rotating frame without CP contact with the protons.

Theoretical Background

Line-broadening mechanisms in glassy polymers have already been reviewed.[6] Some of them, the static ones, i.e., bulk susceptibility of the sample, chemical shift dispersions due to packing effects, bond distortions, and conformational inequivalence, induce only a relatively small effect, $(\pi T_{2res})^{-1}$, on the order of 2–6 ppm. More important are the line broadenings arising from relaxation mechanisms such as motional modulation of the chemical shift anisotropy[7] and motional modulation of the dipolar carbon–proton coupling.[8]

For carbons having a high chemical shift anisotropy, the motional modulation of the chemical shift anisotropy induces a line broadening, $(\pi T_{2\sigma})^{-1}$, that is maximum when the rate of molecular motion is equal to the sample spinning speed.

In the case of carbons having a strong dipolar carbon–proton coupling under suitable conditions of magic-angle setting and proton decoupling irradiation, the main cause of motional line broadening is the modulation of the dipolar ^{13}C–^{1}H coupling. This mechanism gives a maximum line broadening when the rate of molecular motion is equal to the proton decoupling radio-frequency (rf) field strength ω_{1H} expressed in angular frequency units. For slow motions with correlation times in the range 10^{-5}–10^{-7} s, this motional line broadening $(\pi T_{2m})^{-1}$ may be much larger than that due to the previous static effects. Under the conditions that the proton irradiation is applied exactly on resonance and that the sample spinning rate is much smaller than the proton decoupling field strength, the transverse relaxation time resulting from this mechanism and contributing an amount of $(\pi T_{2m})^{-1}$ to the line width is[8]

$$(T_{2m})^{-1} = A_{CH} J(\omega_{1H}) \tag{1}$$

A_{CH} is the part of the carbon–proton second moment that is modulated by the motion and $J(\omega)$ is $J(\omega) = (1/2)\int_{-\infty}^{+\infty} G(t)\, e^{i\omega t}\, dt$, where $G(t)$ is the normalized second-order spherical harmonic autocorrelation function.

In the general case where all mechanisms are effective, the observed full line width at half-height $(\pi T_2)^{-1}$ may be written as

$$\frac{1}{\pi T_2} = \frac{1}{\pi T_{2m}} + \frac{1}{\pi T_{2\sigma}} + \frac{1}{\pi T_{2res}} \tag{2}$$

Molecular motions in the midkilohertz frequency range also provide a strong effect on the spin–lattice relaxation time in the rotating frame. ^{13}C $T_{1\rho}$ is determined by two different mechanisms, one resulting from spin–lattice effects and the other from spin–spin processes:[3,9-13]

$$\frac{1}{^{13}C\ T_{1\rho}} = \frac{1}{^{13}C\ T_{1\rho\ \text{spin-lattice}}} + \frac{1}{T_{CH}(\text{ADRF})} \tag{3}$$

Spin–spin processes come from modulation of the dipolar interactions by the spontaneous rigid-lattice proton spin fluctuations.[3,6,9-13] They are described by the cross-polarization time, $T_{CH}(\text{ADRF})$, in an "ADRF" experiment. Spin–lattice relaxation results from the modulation of internuclear dipolar interactions at the rotating frame Larmor frequency and arises from the same motions which cause the motional line broadening in T_2 measurements. It is maximum when the rate of molecular motion is equal to the carbon spin-locking field strength ω_{1C} expressed in angular frequency units. Under Hartmann–Hahn matching conditions, $\omega_{1H} = \omega_{1C}$, so that ^{13}C $T_{1\rho\ \text{spin-lattice}}$ is equal to T_{2m}:[6,13,14]

$$^{13}C\ T_{1\rho\ \text{spin-lattice}} = T_{2m} \tag{4}$$

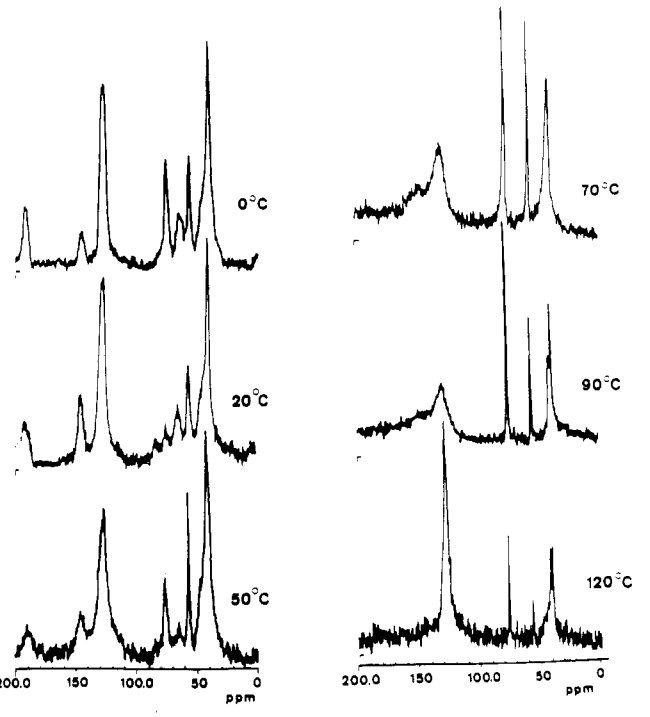

Figure 1. High-resolution solid-state CP/MAS/DD ^{13}C NMR spectra of the 52 wt % PS sample recorded at 75 MHz as a function of temperature, T (contact time: 1 ms).

Results and Discussion

The line assignment obtained from ^{13}C NMR solution spectra is summarized in the following formulas for the PS and PVME units:

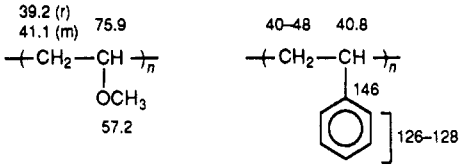

where the positions of the ^{13}C lines are expressed in ppm with respect to TMS.

As an example, the 75-MHz CP/MAS/DD ^{13}C NMR spectra of the 52 wt % PS sample are shown in Figure 1 as a function of temperature. The solid-state ^{13}C chemical shifts are close to the solution ones. However, the lines are broader and the peak observed in the neighborhood of 40 ppm in the ^{13}C NMR solid-state spectra is the sum of four nonresolved lines corresponding to the PVME methylene carbons in the meso and racemic diads and the PS methine carbon and methylene carbon. The resonance of this last carbon appears as a shoulder and is quite wide due to its sensitivity to tactic tetrads. The precise location of the whole set of spinning side bands associated with the PS aromatic carbon resonances can be deduced from the position of the low-field first-order spinning side bands. Superposition of the spinning side bands with the PVME methine carbon line has been avoided as much as possible.

Table I
Glass Transition Temperatures of the Blends (As Measured by DSC), $T_{g\ blend}$, and Temperatures (°C) at Which the Maximum Δ_{O-CH}, Δ_{arom}, and Δ_{chain} Line Broadenings Are Observed for the PVME Methine Carbon and PS Protonated Aromatic and Chain Carbons, Respectively

	38 % wt PS	52 % wt PS	67 % wt PS
$T_{g\ blend}$	-19	-6	19
temp of the max Δ_{O-CH} line broadening	20	29	40
temp of the max Δ_{arom} line broadening	55	75	98
temp of the max Δ_{chain} line broadening			105

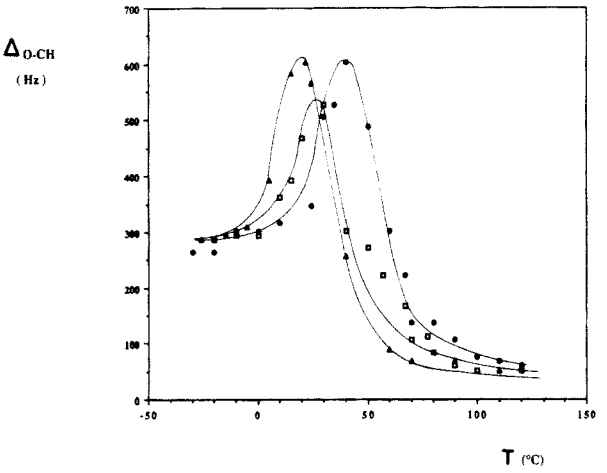

Figure 2. Variation of the 75-MHz Δ_{O-CH} line width as a function of temperature: (▲) 38 wt % PS sample; (□) 52 wt % PS sample; (●) 67 wt % PS sample.

As shown in Figure 1, on increasing the temperature, there is only a small variation in the line shape of the PVME methoxy carbon line which becomes narrower at higher temperatures.

The 40 ppm line, which is the sum of four components, has a complex temperature dependence. The PVME methylene lines are narrow and well-resolved at high temperature.

In contrast, the following behavior is observed for the peaks due to the aromatic carbons of polystyrene and the PVME methine carbons: on increasing temperature, there first occurs a large line broadening and a further decrease of the line width at high temperatures. The values of the maximum line broadenings cannot be determined with a good accuracy because of the presence of adjacent resonances on the spectra. However, the temperatures at which a maximum line broadening occurs are well determined. As shown in Table I, they depend on the carbon line under study and the composition of the blend.

The line widths at midheight, Δ_{O-CH}, measured at 75 MHz for the PVME methine carbon from the CP ^{13}C NMR spectra are reported in Figure 2 for the three blends under study. At high temperature, the measured line widths are independent of the nature (CP or DP) of the pulse sequence used. Besides, in the temperature and composition regions where comparison with Takegoshi and Hikichi's CP and DP ^{13}C NMR experiments[1] can be carried out, the agreement between the two sets of data is very good. Since the CP pulse sequence accentuates the contribution of the most rigid carbons, whereas the direct polarization experiment with long recycle delays leads to the observation of the whole sample with the same contribution from each carbon-13 nucleus, the close similarity of the line widths measured by the two NMR techniques for the PVME methine carbon at high temperatures is significant. It implies that, at these temperatures, the blend samples

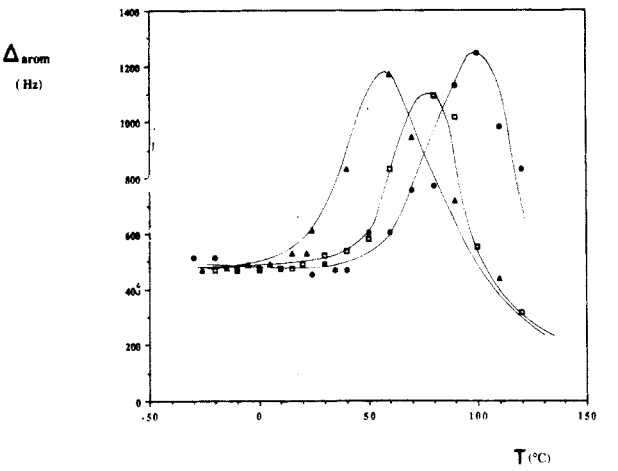

Figure 3. Variation of the 75-MHz Δ_{arom} line width as a function of temperature: (▲) 38 wt % PS sample; (□) 52 wt % PS sample; (●) 67 wt % sample.

are not highly heterogeneous. This point is in agreement with conclusions derived from fluorescence emission and small-angle neutron scattering studies of PS/PVME blends[15,16] that have shown that, at temperatures sufficiently lower than the phase coexistence temperature, T_c, the system fluctuations are low. Composition microheterogeneities in the blends of PS and PVME can only be detected when the samples are subjected to long annealing around T_c -25 °C or above.

The order of magnitude of the maximum Δ_{O-CH} line broadening is beyond the static line broadenings. Therefore, for the PVME methine carbon, which is coupled to a directly bonded proton and whose chemical shift anisotropy is weak, the observed line broadenings can be interpreted in terms of a static contribution and motional modulation of the dipolar carbon-proton coupling. They show the classical $(\pi T_{2m})^{-1} + (\pi T_{2res})^{-1}$ dependence on temperature and frequency of molecular motions and are a clear indication of molecular processes involving the PVME methine carbon with a frequency at the temperature of the maximum line broadening on the order of the strength of the proton decoupling field, i.e., 62.5 kHz. These results are supported by 25-MHz ^{13}C NMR experiments performed on the 38 wt % PS sample. As expected, in these spectra which are recorded at a lower operating frequency, the relative importance of the dynamic line broadening with respect to the static contribution is increased in the temperature range of interest.

The line widths at midheight, Δ_{arom}, determined at 75 MHz from the CP ^{13}C NMR spectra for the PS protonated aromatic carbon lines are shown in Figure 3. As for the PVME methine carbon line widths, experiments performed at high temperature have shown that they are independent of the nature (CP or DP) of the pulse sequence used. The absolute values and temperature dependence of Δ_{arom} cannot be accounted for by static effects only and point out the existence of motions of the PS phenyl rings. However, in this case the precise interpretation of the phenomena is not straightforward, since a protonated aromatic carbon has both quite strong chemical shift anisotropy and dipolar carbon-proton coupling. Therefore, both the motional modulation of the chemical shift anisotropy and motional modulation of the dipolar coupling may be active relaxation mechanisms for this carbon, and maximum line broadenings are expected for motions either on the order of the spinning speed, i.e., 4 kHz, or of the strength of the proton decoupling field, i.e., 62.5 kHz. In this regard, it is of interest to compare the behavior of the

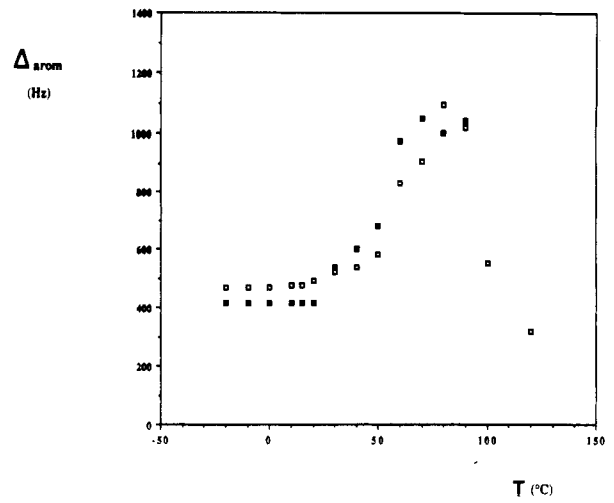

Figure 4. Variation of the 75-MHz line widths of the protonated (□) and nonprotonated (■) aromatic carbons as a function of temperature in the 52 wt % PS sample.

lines assigned to the PS protonated and nonprotonated aromatic carbons since the relative contribution of the modulation of the chemical shift anisotropy to the maximum line broadening is larger for nonprotonated aromatic carbons than for protonated aromatic carbons. Although the accuracy of the measurements of the substituted carbon line width is quite limited, results displayed in Figure 4 clearly show that PS protonated and nonprotonated aromatic carbons have a parallel temperature dependence of their line broadenings with quite similar temperatures at the maximum line broadening. In addition, the line widths of both peaks are quite similar. A likely explanation for such a similarity in the behavior of the protonated and nonprotonated carbon lines is that the motional modulation of the chemical shift anisotropy plays a major role in the line broadening of all the PS aromatic carbon lines. If this is the case, the motions involving the phenyl rings have frequencies in the neighborhood of 4 kHz at the maximum line broadening. However, it must be noted that the conclusions derived in this paper do not depend on the exact nature of the relaxation mechanism. Besides, although these two mechanisms probe motions in somewhat different frequency ranges, this frequency difference corresponds to a temperature difference of only a few degrees, on the order of the accuracy of the determination of the temperature of the maximum line broadening.

In the 1-ms contact time spectra shown in Figure 1, the 40 ppm peak is not resolved so that no information on the behavior of the PS main-chain carbons can be derived. As an example, the ^{13}C NMR spectrum of the 67 wt % PS sample obtained at 90 °C by using a 20-μs contact time is displayed in Figure 5. It shows only two peaks. During such a short contact time only carbons with a strong ^{13}C–^{1}H dipolar coupling, i.e., protonated carbons with a relatively rigid behavior, can acquire some magnetization. Therefore, as confirmed by the values of their chemical shifts, these lines can be readily assigned to the PS protonated aromatic and main-chain carbons. The line widths of the latter carbons have a maximum line broadening which is too large to be due to static effects only. They are broadened by motional modulation of the dipolar carbon–proton coupling. Temperature dependence of the line widths is represented in Figure 6 for the main-chain carbons. It is parallel to the temperature dependence observed for the PS aromatic carbons, with a maximum at a few degrees above the temperature of the Δ_{arom} maximum as expected from the higher (62.5 kHz) obser-

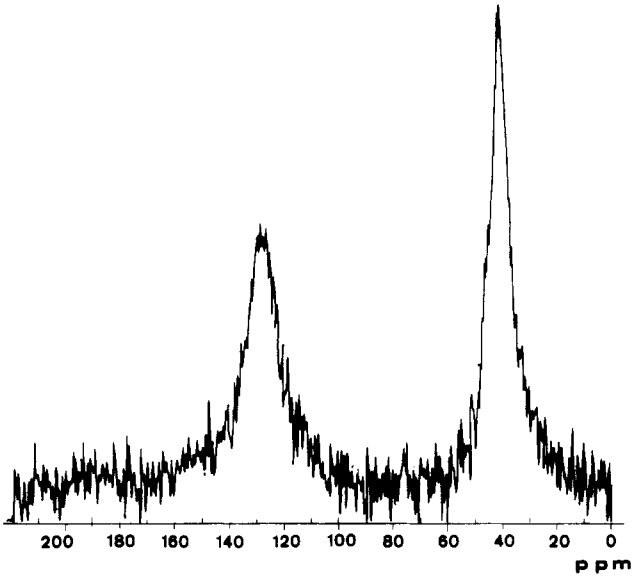

Figure 5. High-resolution solid-state ^{13}C NMR spectrum of the 67 wt % PS sample recorded at 75 MHz and 90 °C by using a contract time of 20 μs.

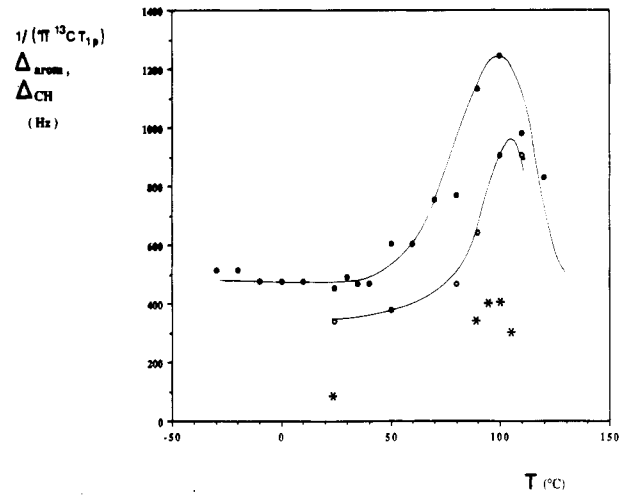

Figure 6. Variation of the 75-MHz line widths of the protonated aromatic carbons (●) and main-chain carbons (○) as a function of temperature in the 67 wt % PS sample and comparison with the temperature dependence of ^{13}C $T_{1\rho}$ (*) for the protonated aromatic carbons in the 67 wt % PS sample.

vation frequency of motions.

The above observations have been complemented by measurements of ^{13}C $T_{1\rho}$. Decreases of the magnetization as a function of the delay time, Δt, have been recorded for the three considered blends. As shown by the example given in Figure 7, they are markedly nonexponential. Such a result has already been observed for polymers and is probably due to the dynamic heterogeneity of these systems.[3] Indeed, in the bulk state, the frequency and amplitude of molecular motions that affect a given type of carbon may vary from place to place, according to the exact strength of the local inter- and intramolecular interactions. As suggested by Schaefer,[3] ^{13}C $T_{1\rho}$ has been derived from the first points ($0 < t \leq 1$ ms) of the magnetization decrease. $1/(\pi\ ^{13}C\ T_{1\rho})$ values thus determined for the protonated aromatic PS carbons are shown in Figure 6. Their absolute values are different from Δ_{arom} values, which is readily understandable since they do not originate from the same relaxation mechanism. However, the temperature dependence of $1/(\pi\ ^{13}C\ T_{1\rho})$ is parallel to that of Δ_{arom} and the $1/(\pi\ ^{13}C\ T_{1\rho})$ and Δ_{arom} maxima are observed at quite the same temperatures. Although ^{13}C $T_{1\rho}$ and Δ_{arom} probe motions in somewhat different

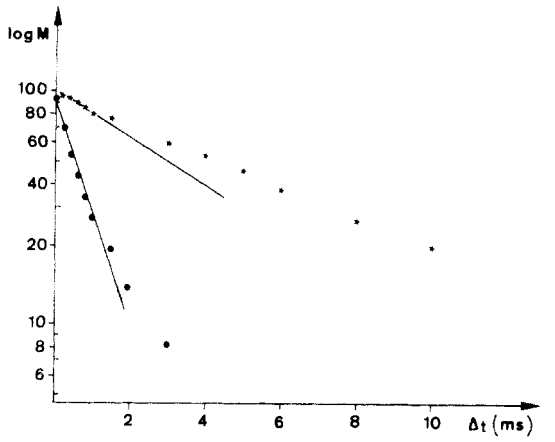

Figure 7. Representative plot of ^{13}C $T_{1\rho}$ data (52 wt % PS sample, 80 °C): (*) PVME OCH carbon, (●) PS protonated aromatic carbons.

frequency ranges (tens of kilohertz and kilohertz ranges, respectively), this frequency difference corresponds to a temperature shift of only a few degrees, so that whatever the relaxation mechanism, the maximum relaxation rate is observed in the same temperature range, within the accuracy of the measurements. This result is a further support of the existence of local PS ring motions in the midkilohertz range in the investigated temperature domain. Parallel behavior of the line widths and $1/(\pi\ ^{13}C\ T_{1\rho})$ as a function of temperature has also been observed for the PVME O–CH and PS main-chain carbons, in agreement with the interpretation of the corresponding line broadenings in terms of local motions.

The results reported above lead to the identification of different types of local modes in the PS/PVME blends. For PVME, the behavior of the methine carbon indicates the existence of local main-chain processes. In the case of PS, the aromatic and main-chain carbon lines have parallel temperature dependence with extrema at very similar temperatures. These observations imply that the PS main chain and side rings are involved in correlated motions. This conclusion is in agreement with results reported on polystyrene in solution and discussed in terms of motions of the main-chain and phenyl rings.[17]

It is of interest to note that the maxima of the line broadenings and $1/(\pi\ ^{13}C\ T_{1\rho})$ values occur at much lower temperatures in the PVME chain than in the PS one. Therefore, although the blends are compatible as proven by the existence of a single glass transition temperature observed by DSC, $T_{g\ \text{blend}}$, and by fluorescence investigation,[2] the PVME and PS chains in the PS/PVME blends do not share the same local chain dynamics at a given $(T - T_{g\ \text{blend}})$ difference. In our experiments, the frequencies of the motions observed for the PS aromatic carbons and PVME methine carbon were centered at about 4 and 62.5 kHz, respectively. For the same observation frequency of 62.5 kHz, the difference in behavior of these two carbons would be still larger. This last point is supported by comparison of the temperature dependences of the line widths associated with the PVME methine carbon (Figure 2) and PS chain carbons (Figure 6), respectively, in the 67 wt % PS sample. The fact that the PVME and PS chains do not share the same local chain dynamics has also been observed by Takegoshi and Hikichi,[1] who have concluded that "the microscopic short-range anisotropic motions for the component polymers are not correlated". Similarly, Miller et al. have shown that, in miscible blends of poly(vinylethylene) and polyisoprene, which do not exhibit chemical interactions, the correlation times for the local motions of the component polymers are different.[18]

Another important point is the dependence of the temperature of the maximum line broadenings on the composition of the blend, which has been demonstrated for the PVME component as well as for the PS component (Table I). This result indicates that the local dynamics of each homopolymer in the blend is not only determined by intramolecular parameters but also depends on intermolecular interactions.

The local motions observed in the range of a few kilohertz or tens of kilohertz in the above experiments occur at temperatures somewhat higher than the glass transition temperature of the compatible blend. Therefore, they are likely related to the motional processes associated with the glass transition phenomena. For homopolymers, the temperature dependence of the correlation times of the motional processes associated with the glass transition phenomenon is well-represented by the Williams–Landel–Ferry (WLF) equation[19] which can be written as[20]

$$\log \frac{\tau_c(T)}{\tau_c(T_g)} = -\frac{C_1^g(T - T_g)}{C_2^g + T - T_g} \tag{5}$$

where $\tau_c(T)$ and $\tau_c(T_g)$ are the correlation times at temperatures T and T_g, respectively. C_1^g and C_2^g can be expressed as

$$C_1^g = \frac{B}{2.303 f_g} \qquad C_2^g = f_g/\alpha \qquad C_1^g C_2^g = \frac{B}{2.303\alpha} \tag{6}$$

where f_g is the fractional free volume at T_g, α the thermal expansion coefficient of the free volume, and $B \sim 1$. Equation 5 can be generalized to any arbitrary reference temperature T_0

$$\log \tau_c(T) = -\frac{C_1^0(T - T_0)}{C_2^0 + T - T_0} + \log \tau_c(T_0) \tag{7}$$

with

$$C_1^0 C_2^0 = C_1^g C_2^g \tag{8}$$

and

$$T_0 - C_2^0 = T_g - C_2^g \tag{9}$$

For polymer blends, the availability of viscoelastic data is limited. In the specific case of PS/PVME blends, the viscoelastic behavior can be represented to some extent by a WLF-type equation.[21] However, the purpose of our study is somewhat different. It does not aim at determining the WLF constants for the blends as a whole, but rather it deals with the behavior of the individual PS and PVME chains inside the blend. In the case of the blend as a whole, the WLF theory is based on mean-field and free-volume considerations. Similarly, the viscoelastic responses of the individual components as a function of temperature are expected to obey a WLF-type equation. However, the dependence of the C_1^g and C_2^g coefficients and $\tau_c(T_g)$ factors on the component and blend composition is still an open question. Therefore, it is of interest to compare the line-width dependence on temperature for both components with the $\tau_c(T)$ dependence which can be written for the PVME chains inside the blend as

$$\log \tau_c(T)_{\text{PVME}} = -\frac{C_{1(\text{PVME})}^g(T - T_{g\ \text{blend}})}{C_{2(\text{PVME})}^g + T - T_{g\ \text{blend}}} + \log \tau_c(T_{g\ \text{blend}})_{\text{PVME}} \tag{10}$$

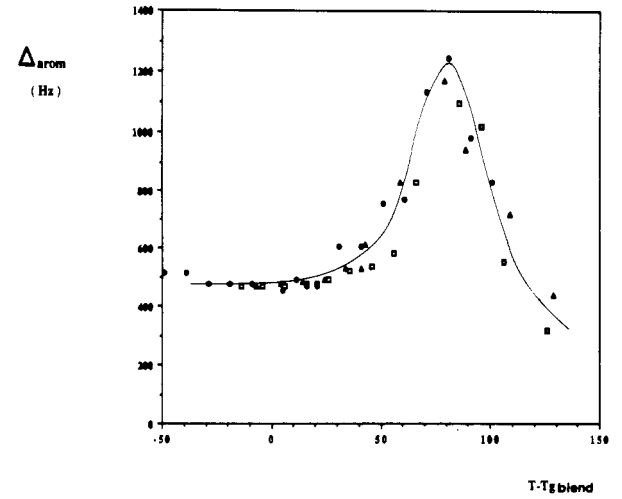

Figure 8. Variation of the 75-MHz Δ_{arom} line width as a function of $(T - T_{g\ blend})$: (▲) 38 wt % PS sample; (□) 52 wt % PS sample; (●) 67 wt % PS sample.

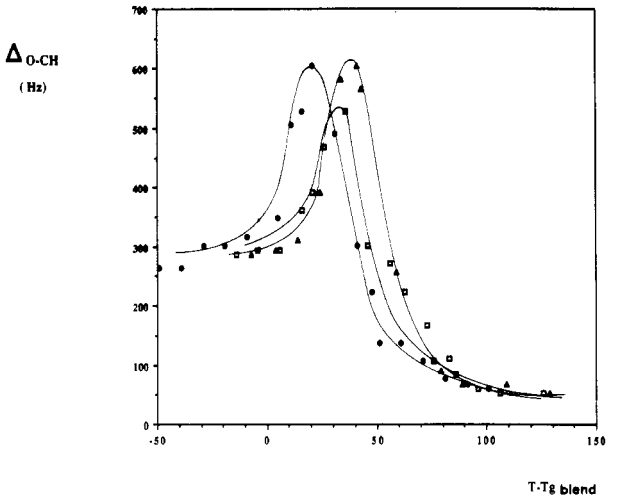

Figure 9. Variation of the 75-MHz $\Delta_{O\text{-}CH}$ line width as a function of $(T - T_{g\ blend})$: (▲) 38 wt % PS sample; (□) 52 wt % PS sample; (●) 67 wt % PS sample.

and for the PS chains inside the blend

$$\log \tau_c(T)_{PS} = -\frac{C^g_{1(PS)}(T - T_{g\ blend})}{C^g_{2(PS)} + T - T_{g\ blend}} + \log \tau_c(T_{g\ blend})_{PS} \quad (11)$$

where $C^g_{1(PVME)}$, $C^g_{2(PVME)}$, $C^g_{1(PS)}$, $C^g_{2(PS)}$, $\tau_c(T_{g\ blend})_{PVME}$, and $\tau_c(T_{g\ blend})_{PS}$ are unknown functions of the blend composition.

Variations of Δ_{arom} and $\Delta_{O\text{-}CH}$ as a function of $(T - T_{g\ blend})$ are shown in Figures 8 and 9. The Δ_{arom} dependence on $(T - T_{g\ blend})$ is identical for the three blends under study, which implies that, within the sensitivity of the ^{13}C NMR experiments, the motions of the PS aromatic carbons can be described by the same values of the $C^g_{1(PS)}$, $C^g_{2(PS)}$, and $\tau_c(T_{g\ blend})_{PS}$ coefficients, independently of the blend composition. As shown in Figures 4 and 6, the broadenings of the PS lines show similar temperature dependences whatever the nature (aromatic or aliphatic, side chain or main chain) of the carbon under consideration. Thus, the local motions of the PS chains in the blends can also be represented by the same values of the $C^g_{1(PS)}$, $C^g_{2(PS)}$, and $\tau_c(T_{g\ blend})_{PS}$ coefficients independently of the blend composition. Therefore, as determined by the local dynamic behavior of the PS chains, the fractional free volume at the glass transition of the blend and the expansion coefficient of the free volume do not depend on the blend composition.

In contrast, the variation with $(T - T_{g\ blend})$ of the PVME $\Delta_{O\text{-}CH}$ line widths depends on the blend considered. At the temperature of the maximum $\Delta_{O\text{-}CH}$ line broadening, the local motions undergone by the PVME methine carbons have the same correlation time whatever the blend composition. It is interesting, therefore, to take the temperature of the maximum line broadening, T_{max}, as the reference temperature, T_0, in eq 7, in order to compare the temperature dependence of the $\Delta_{O\text{-}CH}$ line broadenings in the different blends. Results plotted in Figure 10 show that variations of $\Delta_{O\text{-}CH}$ as a function of $T - T_{max}$ are almost identical for the three blends under consideration. Such behavior implies that the local motions of the PVME chains in the three blends, with these reference conditions, can be described by quite the same values of the WLF coefficients—$C^0_{1(PVME)}$, $C^0_{2(PVME)}$, and $\tau_c(T_0)_{PVME}$—where $T_0 = T_{max}$ depends on the blend composition. These results, combined with the expression in eq 8, lead to the important conclusion that the $C^g_{1(PVME)}C^g_{2(PVME)}$ product is independent of the blend composition.

In spite of the identical values of the $C^g_{1(PVME)} \times C^g_{2(PVME)}$ product, it is important to notice that the value of the differences $(T_{max} - T_{g\ blend})$ varies according to the blend composition (Table I). Rewriting eq 9 as $T_0 - T_g = C^0_2 - C^g_2$, and considering that, at $T_0 = T_{max}$, the values of $C^0_{2(PVME)}$ are independent of the blend composition, yields the conclusion that $C^g_{2(PVME)}$ has to depend on the composition. Use of eq 8 leads to the same conclusion for $C^g_{1(PVME)}$. The latter results imply that the fractional free volume at $T_{g\ blend}$, as detected by the dynamics of the PVME chains, changes with blend composition. According to data reported in Table I, the fractional free volume for the PVME units at the glass transition of the blend would increase with increasing PS content in the blend.

Information regarding the effect of the blend composition on $\tau_c(T_{g\ blend})_{PVME}$ can be obtained by applying the expression in eq 10 at $T = T_0 = T_{max}$:

$$\log \tau_c(T_{g\ blend})_{PVME} = \frac{C^g_{1(PVME)}(T_0 - T_{g\ blend})}{C^g_{2(PVME)} + T_0 - T_{g\ blend}} + \log \tau_c(T_0)_{PVME} = \frac{C^g_{1(PVME)}(T_0 - T_{g\ blend})}{C^0_{2(PVME)}} + \log \tau_c(T_0)_{PVME}$$

Since $\log \tau_c(T_0)_{PVME}$ and $C^0_{2(PVME)}$ are independent of blend composition at $T_0 = T_{max}$, results obtained show that $\tau_c(T_{g\ blend})_{PVME}$ is a decreasing function of PS content, in agreement with data displayed in Figure 9. In other words, when the proportion of PS in the blends increases, the local motions of the PVME chains are faster and faster when the temperature reaches the glass transition of the blend.

The difference in the motional behavior of the PS and PVME chains can be analyzed in terms of the relative sensitivity of the local motions to intramolecular constraints and intermolecular interactions. The fact that the $C^g_{1(PS)}$, $C^g_{2(PS)}$, and $\tau_c(T_{g\ blend})_{PS}$ coefficients are independent of the blend composition would imply that, for the local motions of the PS units, the intramolecular constraints are the dominant factors. On the contrary, for the local motions of PVME chains, the intramolecular contribution is reflected through the faster dynamics of the PVME chains as compared to the PS one. Besides, the composition dependence of the $C^g_{1(PVME)}$, $C^g_{2(PVME)}$, and

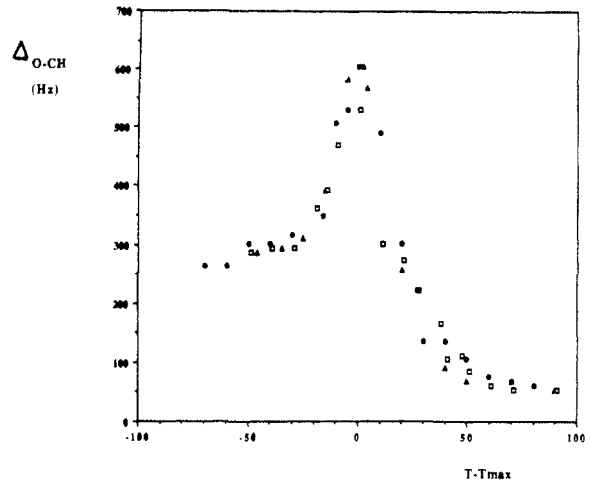

Figure 10. Variation of the 75-MHz $\Delta_{O\text{-}CH}$ line width as a function of $(T - T_{max})$: (▲) 38 wt % PS sample; (□) 52 wt % PS sample; (●) 67 wt % PS sample.

$\tau_c(T_{g\ blend})_{PVME}$ coefficients would indicate a significant effect of the intermolecular interactions.

Conclusion

Variation of the composition in the compatible PS/PVME blends has allowed us to point out the influence of intramolecular constraints and intermolecular interactions on local chain motions. As shown by the broadenings of the resonances observed by high-resolution solid-state ^{13}C NMR, the PS and PVME components do not share the same local chain dynamics. An interesting feature is the difference in the temperature dependence of the local dynamics of the PS and PVME chains as a function of the blend composition. This difference means that the two dynamics have to be described by specific sets of WLF coefficients, $C^g_{1(PS)}$, $C^g_{2(PS)}$, and $\tau_c(T_{g\ blend})_{PS}$ and $C^g_{1(PVME)}$, $C^g_{2(PVME)}$, and $\tau_c(T_{g\ blend})_{PVME}$, respectively. The PS local dynamics appears to be mainly governed by intramolecular constraints, whereas, for the PVME local dynamics, the influence of both intramolecular constraints and intermolecular interactions has been observed.

References and Notes

(1) Takegoshi, K.; Hikichi, K. *J. Chem. Phys.* **1991**, *94*, 3200.
(2) Halary, J. L.; Monnerie, L. *Photophysical and Photochemical Tools in Polymer Science*; Winnik, M. A., Ed.; Reidel Publishing Company: Dordrecht, The Netherlands, 1986; pp 589–610.
(3) Schaefer, J.; Stejskal, E. O.; Buchdahl, R. *Macromolecules* **1977**, *10*, 384.
(4) Stejskal, E. O.; Schaefer, J. *J. Magn. Reson.* **1975**, *18*, 560.
(5) Tegenfeldt, J.; Haeberlen, U.; Waugh, J. S. *J. Magn. Reson.* **1979**, *36*, 453.
(6) VanderHart, D. L.; Earl, W. L.; Garroway, A. N. *J. Magn. Reson.* **1981**, *44*, 361.
(7) Suwelack, D.; Rothwell, W. P.; Waugh, J. S. *J. Chem. Phys.* **1980**, *73*, 2559.
(8) Rothwell, W. P.; Waugh, J. S. *J. Chem. Phys.* **1981**, *74*, 2721.
(9) Stejskal, E. O.; Schaefer, J.; Steger, T. R. *Faraday Soc. Symp.* **1979**, *13*, 56.
(10) Schaefer, J.; Stejskal, E. O.; Steger, T. R.; Sefcik, M. D.; McKay, R. A. *Macromolecules* **1980**, *13*, 1121.
(11) Garroway, A. N.; Moniz, W. B.; Resing, H. A. *Faraday Soc. Symp.* **1979**, *13*, Chapter 6.
(12) VanderHart, D. L.; Garroway, A. N. *J. Chem. Phys.* **1979**, *71*, 2773.
(13) Garroway, A. N.; VanderHart, D. L.; Earl, W. L. *Philos. Trans. R. Soc. London, Ser. A* **1981**, *299*, 609.
(14) Garroway, A. N.; Moniz, W. B.; Resing, H. A. *ACS Symp. Ser.* **1979**, *103*, 67.
(15) Halary, J. L.; Ubrich, J. M.; Monnerie, L.; Yang, H.; Stein, R. S. *Polym. Commun.* **1985**, *26*, 73.
(16) Halary, J. L.; Ben Cheikh Larbi, F.; Oudin, P.; Monnerie, L. *Makromol. Chem.* **1988**, *189*, 2117.
(17) Lauprêtre, F.; Noël, C.; Monnerie, L. *J. Polym. Sci., Polym. Phys. Ed.* **1977**, *15*, 2127.
(18) Miller, J. B.; McGrath, K. J.; Roland, C. M.; Trask, C. A.; Garroway, A. N. *Macromolecules* **1990**, *23*, 4543.
(19) Williams, M. L.; Landel, R. F.; Ferry, J. D. *J. Am. Chem. Soc.* **1955**, *77*, 3701.
(20) Ferry, J. D. *Viscoelastic Properties of Polymers*, 3rd ed.; Wiley: New York, 1980.
(21) Schneider, H. A.; Wirbser, *J. Polym. Prepr. (Am. Chem. Soc., Div. Polym. Chem.)* **1989**, *30*, 1, 54 and references therein.

Registry No. PS (homopolymer), 9003-53-6; PVME (homopolymer), 9003-09-2.